

Article

Global Stabilizing Control of a Continuous Ethanol Fermentation Process Starting from Batch Mode Production

Yuxin Qin  and Chi Zhai * 

Faculty of Chemical Engineering, Kunming University of Science and Technology, Kunming 650500, China; 20212108022@stu.kust.edu.cn

* Correspondence: zhaichi@kust.edu.cn

Abstract: Traditional batch ethanol fermentation poses the problems of poor production and economic viability because the lag and stationary phase always demand considerable fermentation time; plus, downtime between batches is requested to harvest, clean, and sterilize, decreasing the overall productivity and increasing labor cost. To promote productivity and prolong the production period, avoid process instability, and assure a substantial production of ethanol and a minimal quantity of residual substrate, this paper proposed a nonlinear adaptive control which can realize global stabilizing control of the process starting from batch mode to achieve batch/washout avoidance. Due to the dynamic nature and complexity of the process, novel estimation and control schemes are designed and tested on an ethanol fermentation model. These schemes are global stabilizing control laws including adaptive control to avoid input saturation, nonlinear estimation of the unknown influential concentration through a higher-order sliding mode observer, and state observers and parameter estimators used to estimate the unknown states and kinetics. Since the temperature is an important factor for an efficient operation of the process, a split ranging control framework is also developed. To verify the process performance improvement by continuous fermentation, tests performed via numerical simulations under realistic conditions are presented.

Keywords: adaptive control; washout/batch avoidance; observer-based estimation; fermentation control



Citation: Qin, Y.; Zhai, C. Global Stabilizing Control of a Continuous Ethanol Fermentation Process Starting from Batch Mode Production. *Processes* **2024**, *12*, 819. <https://doi.org/10.3390/pr12040819>

Academic Editor: Antoni Sanchez

Received: 23 March 2024

Revised: 14 April 2024

Accepted: 17 April 2024

Published: 18 April 2024



Copyright: © 2024 by the authors. Licensee MDPI, Basel, Switzerland. This article is an open access article distributed under the terms and conditions of the Creative Commons Attribution (CC BY) license (<https://creativecommons.org/licenses/by/4.0/>).

1. Introduction

With the growth of the bio-manufacturing industry, the design of bio-conversion systems has drawn considerable attention due to their potential to improve production efficiency, plant profitability, and sustainability [1,2]. As a renewable source of fuel, ethanol represents a great opportunity to help meet future energy demands and reduce greenhouse gas (GHG) emissions. Consequently, the production of ethanol has been attracting plenty of interest from all over the world, especially with the breakthroughs in the pretreatment and enzymatic hydrolysis of lignocellulosic feed-stocks that hold an annual yield of about 180 billion tons [3] worldwide.

Despite well-recognized technical barriers to viable commercialization of bio-ethanol having been overcome, the fermentation process itself is now identified as a limiting factor and poses a multi-scale challenge. First of all, current fermentation is mainly batch/fed-batch based, which demands intensive labor for both prior- and post-production; plus, the lag and stationary phase occupies considerable time, causing relatively low productivity. The second challenge is on the design of suitable mathematical models to describe this complex bioprocess; and because bioprocesses use living microorganisms that act as biocatalysts, they are sensitive to extracellular environment, and obtaining accurate and reasonably priced sensors for real-time measurement of the bioprocess variables utilized in the control systems is problematic [4–6]. Moreover, appropriate design of the regulator demands strict and multidimensional defining of critical process parameters for the used microorganism strain, but start-up or maintaining the bioreactor is a long-term

process during which objectives, physicochemical variables, and dynamic behavior can be changed by the operator. Nonetheless, the International Energy Agency [7] forecasts that in 2050, 27% of the global transport fuel can be sustainably supplied from biomass and waste resources. As a result, the ethanol fermentation process design and optimization are inherently synergistic and multidisciplinary.

The design of the fermentation configuration is expected to improve metabolic intensity, increase productivity, and accelerate substrate conversion. Correspondingly, continuous culturing eliminates downtime between batches, as well as the requested interval to harvest, clean, and sterilize; hence, this intensifies production and reduces labor cost. By chemostats or turbidostats, a continuous culture device dilutes cells and waste products at the same rate that they are being produced. But a typical drawback of the continuous fermentation is the presence of multiple outputs (which would easily shift the process to the washout condition), as well as oscillations under certain conditions (the effect being the decrease in ethanol productivity, the loss of a high quantity of substrate). To stabilize the process, the cause of the reactor instability [8–12] is investigated; and, in view of the fact that the osmotic pressure formed at high ethanol concentrations (~50–60 g/L [13,14]) might inhibit or even kill yeast cells, hybrid designs through *in situ* ethanol removal to alleviate ethanol stress [15] are proposed. However, the accompanied instrumental cost as well as possible membrane fouling and degeneration are unbearable in industry.

On the other hand, formulating a feedback control loop through manipulating dilution rate, dissolved oxygen level, pH, or inlet substrate concentration [16–23] to eliminate the fermentation–separation mismatch is a cost-effective way to stabilize the process. The research in this domain is oriented both to the developing of suitable mathematical models and to the design of appropriate monitoring and control strategies able to assure the stability. To summarize, the ethanol fermentation process is influenced by a number of parameters, such as temperature, substrate, pH value, fermentation time, mixing speed, and inoculum size, as well as the concentration of ethanol in the system [24]. Hence, the system to control is multidimensional and complex, and their models contain kinetic parameters that are uncertain and time-varying. A number of stabilization techniques necessitate software sensors for the estimation of biological states, kinetic parameters, and even kinetic reactions based on detectable signals. However, the estimation of input substrate concentration is a difficult task in practice, the input conditions are unknown and time-varying because of upstream disturbances, especially for the continuous production mode where a series of CSTR tanks are connected to decrease the overall substrate run-off.

Observer-based estimation of the fermenter states and kinetics with limited on-line measurements and knowledge of the process model information could minimize the capital cost of the formulated closed-loop system, but process–model mismatch is an in-avoidable factor. Moreover, the control objectives become fuzzy as the main biological state variables vary extremely slowly; for instance, the duration of one batch fermentation that account for 87% of the world ethanol production scale is about 60–72 h, where almost no control intervention is added in classic flow-sheet. To clarify the objectives to control, intensive experimental and theoretical research [25] applications concentrate on growing cultures under different conditions in order to properly characterize the microorganisms and to find optimum productivity. To make the most profit from the process, it is also demanded to minimize the transition time between consecutive steady state operating points. For this reason, global stability is essential for their successful control.

To approach maximum metabolic intensity, this paper works on global stabilizing control (GSC) of the fermentation process which starts from batch mode, and the control is implemented to prolong the production period, where the ladder pattern trajectory of substrate concentration is tracked to approximate toward the unknown substrate consumption capabilities. Previously reported GCS approaches are mainly linearizing controllers [26], but the main drawback of these global approaches is that they use perfect model knowledge. Other global control techniques assuming model uncertainties arise [27], using interval observers' results. However, a drawback common to most of the aforementioned control

strategies is that they often do not explicitly take into account the non-negativity constraints on the manipulated variables.

In this paper, a globally adaptive feedback law is adopted that the feedback gain dynamically adapted in such a way that control never saturates, and the unknown input substrate concentration is explicitly related in the control law to accommodate the time-varying disturbance. For reconstructing the unknown states and disturbed input concentration information from the measurements of ethanol and substrate concentrations, a sliding-mode observer (SMO) is derived. The design of state observers and parameter estimators depends on the information provided on-line by the previous. The distinguishing properties of the discontinuous generalized super-twisting observer (GSTO) compared to other smooth observers are convergence in finite time and insensitivity to time-varying but bounded perturbations [28].

The paper is organized in the following manner. Section 2 describes the fermentation process model, and possible monitoring/control problems under different operation modes are discussed; this is followed by the development of adaptive estimation and control in Section 3; in Section 4, experiment validation is conducted on the ethanol fermentation process, and adaptive control under unknown inputs and undetectable states is implemented in this MIMO system, where to obtain optimal state references the system starting in batch mode is regulated using the technique of global stabilizing control; finally, Section 5 concludes the paper.

2. Problem Formulation

In this paper, a continuous fermentation process of *Saccharomyces cerevisiae* used to produce ethanol is studied; subsequent investigation on batch mode production is realized by manipulating input/output flow rates (or dilution rate) synchronously. As is shown in Figure 1, a flow F_{in} of culturing broth containing substrate S_{in} is continuously fed into the reactor, the volume V is held constant when the outflow $F_{out} = F_{in}$. The jacket with control (V_j, T_{inj}, F_j) could maintain the reactor temperature T_r as desired. We assume the content is well-mixed with one substrate-limited material (e.g., glucose) feeding in continuously for the growth of biomass/yeast, and the same amount of broth liquor is removed to acquire the product ethanol.

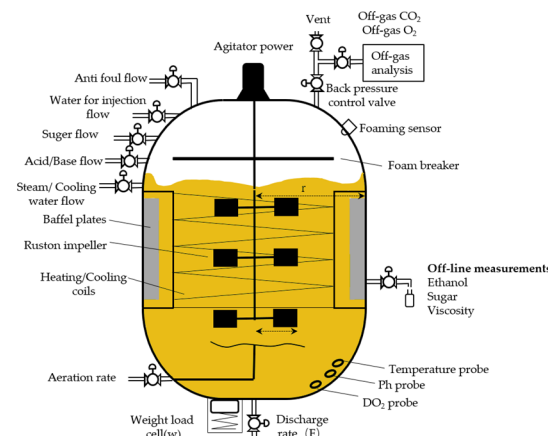


Figure 1. Schematic of the bioreactor equipped with a jacket.

The nonlinear dynamics of the studied process [29] in Figure 1 can be obtained based on the mass balance of the substrate (S), biomass (X), and product (P) as follows,

$$\left\{ \begin{array}{l} \frac{dS}{dt} = D(S_{in} - S) - \frac{r_1}{Y_{SX}} - \frac{r_2}{Y_{SP}} \\ \frac{dX}{dt} = -DX + r_1(\mu_m(\cdot), S, P, X) \\ \frac{dP}{dt} = -DP + r_2(\mu_P, S, X, P) \\ S(0) = S_{in}, X(0) = X_0, P(0) = P_0 \end{array} \right. \quad (1)$$

where $F_{in} = F_{out} = F$, and $D = F/V$ is the dilution rate defined as the reciprocal of the reactor space–time for the culturing media, which is the control action used to determine the operating status of the chemostat. One crucial problem in solving Equation (1) is the formulation of expressions for the kinetic functions $r_1(\cdot)$ and $r_2(\cdot)$, which could be a large number of analytical expression candidates. Note that in practical applications, actuators could be adopted to create the control action D , and their dynamics will be considered in Section 4.1.

In practice, fermenter control design should consider realistic conditions related to process inputs, state variables, and reaction kinetics, as well as possible control to enhance substrate conversion and the production rate. Without a loss of generality, the following performance requirement and assumption are considered.

1. Monitoring Information: The quantity $r_2(\cdot)$ is available on-line from the plant, and for a large part of bioprocesses, the production (or consumption) of gaseous components, as peculiar to ethanol fermentation by *S. cerevisiae*, CO_2 is monitored and is directly related to $r_2(\cdot)$, and the accumulation of CO_2 evolution rate (CER) is proportional to P when D is fixed.
2. Dynamic Heat Balance of the Jacketed Fermenter: In order to assure a hospitable environment, fermentation temperature is regulated to maintain at an optimum. The aerobiotic respiration effect might cause exothermic reactions and a jacket cooler is integrated to remove redundant heat, and heat transfer between the broth and coolant is rendered as perfect convection,

$$\begin{cases} \frac{dT_r}{dt} = D(T_{in} - T_r) + \frac{\Delta H_r \cdot r_{O_2}}{32 \cdot \rho_r \cdot C_{heat,r}} - \frac{K_T A_T (T_r - T_j)}{V \cdot \rho_r \cdot C_{heat,r}} \\ \frac{dT_j}{dt} = D_j(T_{inj} - T_j) + \frac{K_T A_T (T_r - T_j)}{V_j \cdot \rho_j \cdot C_{heat,j}} \\ \frac{dO_2}{dt} = K_L a_0 \cdot 1.024^{(T_r - 20)} (O_2^{sat} - O_2) - r_{O_2} - DO_2 \\ T_r(0) = T_{r0}, T_j(0) = T_{inj}, O_2(0) = O_2^{sat} \end{cases} \quad (2)$$

where ΔH_r is the mole enthalpy change in the oxidation reaction; $K_T A_T$ is the heat transfer coefficient multiples area of heat exchange. Note that O_2 from the sterilized air is dissolved into the broth and transported by input effluents, and the aerobiotic effect of yeast leads to exothermic reactions. Dissolved oxygen (DO) content in the electrolyte solution is influenced by pH, T_r , and the global effect of ionic strength $\sum H_k I_k$,

$$O_2^{sat} = f(T_r) \cdot 10^{-\sum H_k I_k} \quad (3)$$

where $\sum H_k I_k$ is accounted as [28,29] follows,

$$\begin{aligned} \sum H_k I_k = & 0.5 H_{Na} \frac{m_{NaCl}}{M_{NaCl}} \frac{M_{Na}}{V} + 2 H_{Ca} \frac{m_{CaCO_3}}{M_{CaCO_3}} \frac{M_{Ca}}{V} + 2 H_{Mg} \frac{m_{MgCl_2}}{M_{MgCl_2}} \frac{M_{Mg}}{V} \\ & + 0.5 H_{Cl} \left(\frac{m_{NaCl}}{M_{NaCl}} + 2 \frac{m_{MgCl_2}}{M_{MgCl_2}} \right) \frac{M_{Cl}}{V} + 2 H_{CO_3} \frac{m_{CaCO_3}}{M_{CaCO_3}} \frac{M_{CO_3}}{V} \\ & + 0.5 H_H 10^{-pH} + 0.5 H_{OH} 10^{-(14-pH)} \end{aligned} \quad (4)$$

3. Temperature influence on the kinetics: The maximum specific growth rate μ_m is correlated with the broth temperature which is provided in the form of the Arrhenius formula,

$$\mu_m = A_1 e^{\frac{-E_{a1}}{R(T_r + 273)}} - A_2 e^{\frac{-E_{a2}}{R(T_r + 273)}} \quad (5)$$

where E_{a1} and E_{a2} are the activation energy, and A_1 and A_2 are the preexponential factors.

Remark 1. Systems (1)–(5) have been widely used to represent essential characteristics of the continuous fermentation process. Some advanced controllers have been proposed to regulate temperature and the states [30] and references therein. However, fermentation is an accumulative process where the substrate conversion rate/productivity is extremely slow, prescribed set-point tracking is challenged both on stability of the control law, as well as the adequacy for productivity increase. In view that there exists a maximum handling capability for microorganisms, the control objective of the chemostat is set as the ladder pattern, and the fermentation starts as batch mode and by so tracking, the period is prolonged to intensify productive, and by trial-and-error, maximum substrate conversion capability is obtained. To realize such a control, GSC is mandatory.

Remark 2. Controlling tends to stabilizing, and a primary tool for culturing cells in a static environment is continuous culture, where inoculated growth medium is continually diluted with fresh medium. At steady state, a continuous culture device will dilute cells and waste substrates at the same rate that they are being produced leading to an unchanging environment [31]. To alleviate substrate run-off, industrial practice adopts CSTRs in series, and the input state S_{in} for a given fermenter becomes unknown and time-varying, biomass content X is not measurable on-line, and the biomass growth rate $r(\cdot)$ is completely unknown and time-varying because of uncertainties related to the maximum specific growth rate μ_m and of unavailability of X. Moreover, the control expects ethanol concentration and substrate conversion rate, as well as bio-conversion rate to be optimal, but non-linearity of the process might drive the system to washout condition and terminates the fermentation process. Hence, adaptive control related to the optimal status is to be achieved. It should be noted that X, r_{O_2} , and $r_1(\cdot)$ are nonlinear and also unknown in this paper, which will be estimated on-line with observers.

3. Controller and Estimator Design

In this section, a GSC is proposed for (1) and (2) to regulate fermentation states and temperature. The optimal control of fermentation states is realized through the shifting of batch mode to continuous mode production; and, by ladder pattern trajectory tracking, the maximum substrate conversion rate of the fermenter is obtained and controlled. For the control of temperature, feedback linearization is adopted because we render measurement and modeling of the fermenter temperature which is corrected. Both above-mentioned controls need to consider bioreactor requirements like DO content, biomass X, and the time-varying substrate input concentration S_{in} .

3.1. Global Stabilizing Control

Demanding on the control purpose, we want to globally regulate the fermentation states $[S, X, P]$, but ethanol is viewed as primary metabolite and the kinetics r_1 and r_2 becomes correlative, which leads the values of X and P obtained at equilibrium are completely determined by the value of the targeted set point S^{ref} for substrate concentration. Then, we will only focus on regulation of S in this work.

$S^{ref} \in (0, S_{in})$ denotes the desired set points; the corresponding positive equilibrium values are $P^{ref} = r_2 Y_{SX} Y_{SP} (S_{in} - S^{ref}) / (r_1 Y_{SP} + r_2 Y_{SX})$ and $X^{ref} = r_1 Y_{SX} Y_{SP} (S_{in} - S^{ref}) / (r_1 Y_{SP} + r_2 Y_{SX})$. The objective is to formulate a control $D(\cdot)$ to globally stabilize (1) towards the reference $[S^{ref}, P^{ref}, X^{ref}]$. We set $\beta = r_1/r_2$, and the nonlinear control law is obtained,

$$D(\cdot) = \frac{r_2(\cdot)}{S_{in} - S^{ref}} \left(\frac{\beta}{Y_{SX}} + \frac{1}{Y_{SP}} \right) \quad (6)$$

which formulates the following closed-loop system,

$$\begin{cases} \frac{dS}{dt} = D(\cdot)(S^{ref} - S) \\ \frac{dX}{dt} = D(\cdot)(X^{ref} - X) \\ \frac{dP}{dt} = D(\cdot)(P^{ref} - P) \end{cases} \quad (7)$$

Since $[S, X, P]$ is positively invariant, for any initial state conditions with physical meaning, the control $D(\cdot) \geq 0$, integrating Equation (7), and we show that for any $t \geq 0$,

$$\begin{aligned} \max(X^{ref}, X(0)) &\geq X(t) \geq \min(X^{ref}, X(0)) > 0, \\ \max(S^{ref}, S(0)) &\geq S(t) \geq \min(S^{ref}, S(0)) > 0. \end{aligned} \quad (8)$$

Hence, the control law (6) is bounded below by a positive constant; plus, (7) provides $[S^{ref}, P^{ref}, X^{ref}]$ as globally exponentially stable. To mention, (6) is the nonlinear control that is difficult to realize through error $dS = S^{ref} - S$ reduction, and the linearization control of a chemostat based on (6) towards any a set-point S^{ref} , even unreachable in open-loop, is also globally stabilizable, which is similarly rephrased by the following fermenter temperature control.

In this paper, we adopt the linearization control of fermenter temperature using jacket flow F_j as the manipulated variable. We assume the model (2) is precise and full knowledge of temperature measurement is available. Firstly, given that the jacket volume V_j is orders smaller than the fermenter volume V , the quasi-steady state obtains,

$$T_r - T_j = \frac{\rho_j \cdot C_{heat,j}}{K_T A_T} (T_{inj} - T_j) \cdot F_j \quad (9)$$

which substituted in the first formula gives

$$\dot{T}_r(t) = \frac{F_{in}}{V} (T_{in} - T_r) + \frac{\Delta H_r r_{O_2}}{32\rho_r C_{heat,r}} - \frac{\rho_j C_{heat,j}}{V \rho_r C_{heat,r}} (T_{inj} - T_j) \cdot F_j \quad (10)$$

and by the form of variation, Equation (10) provides the transfer relation,

$$\delta \dot{T}_r(t) \approx -\frac{\rho_j C_{heat,j}}{V \rho_r C_{heat,r}} (T_{inj} - T_j) \cdot \delta F_j \quad (11)$$

where $\delta T_r = T_r^{ref} - T_r$. Moreover, the equilibrium at the reference provides,

$$\frac{F_{in}}{V} (T_{in} - T_r^{ref}) + \frac{\Delta H_r r_{O_2}}{32\rho_r C_{heat,r}} - \frac{\rho_j C_{heat,j}}{V \rho_r C_{heat,r}} (T_{inj} - T_j) \cdot F_j^{ref} = 0 \quad (12)$$

We replace Equation (10) with Equations (11) and (12) and the exact linearization control gives,

$$F_j(t) = F_j^{ref} + \Delta F_j = \frac{\rho_r C_{heat,r}}{\rho_j C_{heat,j}} \frac{V}{T_{inj} - T_j} \left(\dot{T}_r^{ref} - \dot{T}_r(t) - \frac{\Delta H_r r_{O_2}}{32\rho_r C_{heat,r}} - D(T_{in} - T_r) \right) \quad (13)$$

Eliminating the derivatives, we have the control law as follows,

$$F_j(t) = \frac{\rho_r C_{heat,r}}{\rho_j C_{heat,j}} \frac{V}{T_{inj} - T_j} \left(\eta (T_r^{ref} - T_r) - \frac{\Delta H_r r_{O_2}}{32\rho_r C_{heat,r}} - D(T_{in} - T_r) \right) \quad (14)$$

The closed-loop system adopting Equation (14) provides,

$$\left(\dot{T}_r^{ref} - \dot{T}_r \right) + \eta \cdot (T_r^{ref} - T_r) = 0 \quad (15)$$

and when the tuning parameter η is positive, the closed-loop system is globally stabilizable.

Remark 3. Regulating the chemostat by the following linearization control is also globally stabilizable,

$$D(\cdot) = \frac{r_2(\cdot)}{S_{in} - S} \left(\eta_1 (S^{ref} - S) + \frac{\beta}{Y_{SX}} + \frac{1}{Y_{SP}} \right) \quad (16)$$

However, the controller proposed in (16) requires perfect knowledge of the dynamic system, and an adaptive feedback control law based on on-line information from the plant is provided.

Theorem 1. Assume the kinetics r_2 is monitored on-line by CER and follows $y_1 = \lambda r_2$, the adaptive control law,

$$\begin{aligned} D(\cdot) &= \gamma(t)y_1 = \gamma(t)\lambda r_2(S, X, P \dots) \\ \gamma' &= Ky_1(S^{ref} - S)(\gamma - \gamma_m)(\gamma_M - \gamma) \\ \text{with : } &\gamma_M > \gamma^{ref} > \gamma_m > \left(\frac{\beta}{Y_{SX}} + \frac{1}{Y_{SP}}\right)/(\lambda S_{in}) > 0 \text{ and } K > 0 \end{aligned} \quad (17)$$

globally stabilizing (1) towards the positive set points $[S^{ref}, P^{ref}, X^{ref}, \gamma^{ref}]$, where $\gamma^{ref} = (\beta/Y_{SX} + 1/Y_{SP})/\lambda/(S_{in} - S^{ref})$.

Proof. Control law (17) yields to the closed-loop system,

$$\begin{cases} \frac{dS}{dt} = y_1 \left[\gamma(S_{in} - S) - \left(\frac{\beta}{Y_{SX}} + \frac{1}{Y_{SP}} \right) / \lambda \right] \\ \frac{dX}{dt} = y_1(\beta/\lambda - \gamma X) \\ \frac{dP}{dt} = y_1(1/\lambda - \gamma P) \\ \frac{d\gamma}{dt} = Ky_1(S^{ref} - S)(\gamma - \gamma_m)(\gamma_M - \gamma) \end{cases} \quad (18)$$

Consider the positive initial condition plus $\gamma(0) \in (\gamma_m, \gamma_M)$; then, γ is bounded similar to (8),

$$\max(\gamma_M, \gamma(0)) \geq \gamma(t) \geq \min(X_m, \gamma(0)) > 0. \quad (19)$$

Since $y_1 = \lambda r_2$ is bounded below a positive constant, a time change $\tau = ty_1$, and obtains the following standard control,

$$\begin{cases} \frac{dX}{d\tau} = \beta/\lambda - \gamma X \\ \frac{dP}{d\tau} = 1/\lambda - \gamma P \\ \frac{dv}{d\tau} = \gamma^{ref} v^{ref} - \gamma v \\ \frac{d\gamma}{d\tau} = K(v - v^{ref})(\gamma - \gamma_m)(\gamma_M - \gamma) \end{cases} \quad (20)$$

where $v^{ref} = S_{in} - S^{ref}$. Since (20) is an autonomous triangular system, it is separable [32], and for the subsystem in v and γ , the initial condition is confined to the set $W = \{v > 0, \gamma \in (\gamma_m, \gamma_M)\}$; then, an analog can be performed that v is viewed as the prey and γ as the predator, and the Lyapunov function is formulated,

$$V(v, \gamma) = \int_{v^{ref}}^v \frac{x - v^{ref}}{x} dx + \int_{\gamma^{ref}}^{\gamma} \frac{y - \gamma^{ref}}{K(y - \gamma_m)(\gamma_M - y)} dy \quad (21)$$

We check that $V(v, \gamma)$ is defined, non-negative on W , and vanishes only on $v = v^{ref}$ and $\gamma = \gamma^{ref}$, and

$$V' = -\left(\gamma^{ref}(v^{ref} -)^2/v\right) \quad (22)$$

which is non-positive. From Lasalle's theorem, (v^{ref}, γ^{ref}) is a globally attractive fixed point, and so are (X^{ref}, P^{ref}) , considering that (20) is the triangular system. Thus, moving back to the original time and state variables, the control law (17) globally stabilizes the system (1) towards the nominal reference represented by S^{ref} . \square

Remark 4. In addition to the information of CER, control (17) also demands the substrate (glucose) content available on-line, which could be detected in real time using automated approaches, like near-infrared, Fourier transformed infrared and Raman spectroscopy, or soft sensors [33,34]. The detection of $r_2(\cdot)$ is challenging, but for a large part of bioprocesses, the production/consumption of

gaseous components (dissolved oxygen, CO_2) is monitored and is directly related to kinetics. For yeast cell growth, CO_2 is usually released from the fermenter as a by-product, and this makes CER another feedback control parameter for the control system, defined as follows,

$$\text{CER} \left[\frac{\text{mol}}{\text{L} \cdot \text{h}} \right] = \frac{P}{RTV} Q (\text{CO}_2\text{gasout} - \text{CO}_2\text{airinput}) \quad (23)$$

where P is the pressure (atm), R is the ideal gas constant ($\text{atm}\cdot\text{L}/(\text{mol}\cdot\text{K})$), T is the temperature of the venting gas mixture (K), V is the working volume of the liquid inside the fermenter (L), Q is the volumetric gas flow rate for the existing gas stream (L/h), CO_2 gas out is the gaseous CO_2 concentration read by a near-infrared sensor in the venting line of a fermenter, and CO_2 air input is the gaseous CO_2 concentration obtained from the constant air flow.

Remark 5. The above control (17) is implemented on a chemostat where the substrate is measured and controlled; if the system is designed to regulate cell content X by turbidostats with the aid of an on-line OD_{600} sensor, we can build the adaptive control as follows,

$$\gamma' = K(x - x^{\text{ref}})(\gamma_m - \gamma)(\gamma_M - \gamma) \\ \text{with : } 0 < \frac{k}{\lambda s_{in}} < \gamma_m < \frac{1}{\lambda \alpha x^{\text{ref}}} < \gamma_M \text{ and } K > 0$$

Similarly, the regulation of P can also be developed with the same kind of adaption.

3.2. Observer-Based Estimation

Taking in account the whole knowledge concerning the process, the realistic conditions related to inputs, states, and reaction kinetics are listed in Figure 2: the input substrate concentration S_{in} is unknown and time-varying; the process state variable X is not measurable; the biomass growth rate $r_1(\cdot)$, production rate $r_2(\cdot)$, and oxygen consumption rate $r_{O_2}(\cdot)$ are unknown and time-varying because of uncertainties related to the maximum specific growth rate μ_m and X ; the variables S , P , and CER are available on-line; the temperatures T_{in} and T_{inj} are time-varying.

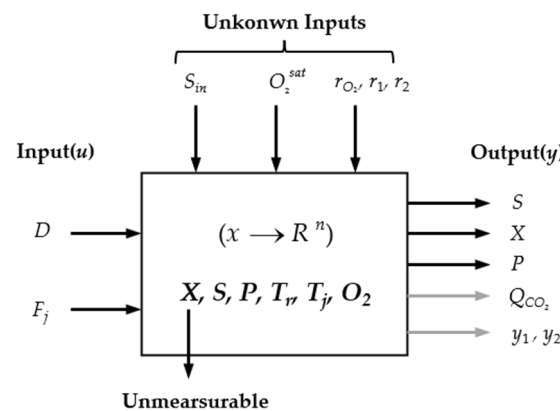


Figure 2. Diagram of the plant information.

3.2.1. Estimation of the Input Substrate Concentration

To facilitate the control of fermentation states, the input information S_{in} in (17) is mandatory, which might be unknown and time-varying when shifting to continuous mode. To alleviate residual substrate loss and upgrade ethanol content, common industrial practice adopts cascade fermentation with a series of tanks and partial reuse of end effluent, as is shown in Figure 3. For one casually assigned medial fermenter i in the series, problems arise as the input S_{in} is influenced by both upstream effluent and the supplement, causing the feed to be unknown and time-varying. Plus, it is assumed that the optimal set-point S_{in}^{ref} is a function of S_{in} (since bio-conversion intensity is relatively constant for a given cell environment); hence, the reference might be time-varying if optimal operation of the

process is expected. Hence, for the control of a fermenter i (labeled with red box), S_{in} is both unknown and time-varying, even S_{in} from saccharification section is fixed.

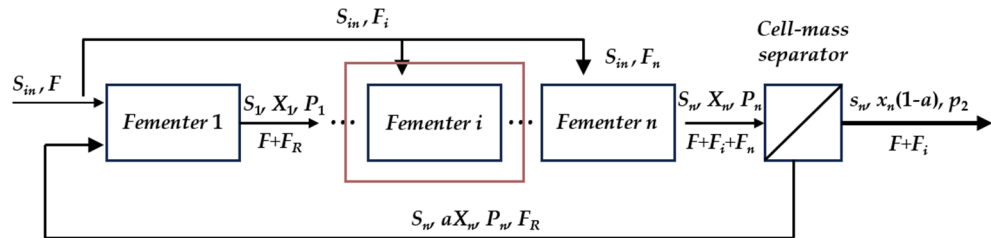


Figure 3. Continuous ethanol fermentation flow-sheet and the corresponding state relations. Continuous fermentation with bio-reaction tanks in series, with partial reuse of the yeast cell separation; ethanol production efficiency increases, and the series of reactors form a gradient decline in substrate content loss.

Based on the assumptions given in Figure 2, the estimation of the input substrate concentration is proposed. Firstly, $\psi = S + P/Y_{XP} + X/Y_{XS}$ is constructed which gives $d\psi/dt = D(-\psi + S_{in})$. Clearly, the auxiliary variable ψ is highly correlated with S_{in} through mass balance,

$$S_{in} \equiv S + \delta X/Y_{XS} + \delta P/Y_{XP} \quad (24)$$

with : $\delta X = X - X_0$, $\delta P = P - P_0$

and when the initial states X_0 and P_0 approach zero, ψ and S_{in} are identical. From the state estimation perspective, the varying of S_{in} because of upstream disturbance could be reflected by changes in the time-derivative of ψ , and one can adopt observer-based estimation (OBE) on S_{in} through ψ .

Assuming ψ is available on-line, a linear observer is shown,

$$\begin{cases} \frac{d\hat{\psi}}{dt} = -D\psi + D\hat{S}_{in} - \kappa_1\lambda_\psi(\hat{\psi} - \psi) \\ \frac{d\hat{S}_{in}}{dt} = -\kappa_2\lambda_\psi^2(\hat{\psi} - \psi) \end{cases} \quad (25)$$

With appropriately designed gains $\kappa_1 > 0$, the parameters $\kappa_2 > 0$ and $\lambda_\psi > 0$ are known to provide an exponentially convergent estimate of S_{in} in the absence of unknown perturbations. However, strict equivalence of S_{in} and ψ is inappropriate in practice and the deviation is manifested as unknown inputs. In synthesis, the linear observer (25) is not able to converge to the true value of the unmeasured states in the presence of unknown inputs. In fact, finite-time convergence is impossible for any observer having locally Lipschitz continuous perturbations, and convergence in the presence of persistent unknown inputs is also impossible for any continuous observer.

In order to alleviate the problem, SMO is introduced for trade-off of the perturbation terms, and to further estimate S_{in} correctly and obtain the convergent effect in finite time, the GSTO technique is adopted,

$$\begin{cases} \frac{d\hat{\psi}}{dt} = -D\psi + D\hat{S}_{in} - \kappa_1\lambda_\psi\phi_1(\hat{\psi} - \psi) \\ \frac{d\hat{S}_{in}}{dt} = -\kappa_2\lambda_\psi^2\phi_2(\hat{\psi} - \psi) \end{cases} \quad (26)$$

with : $\begin{cases} \phi_1(\hat{\psi} - \psi) = \mu_1|\hat{\psi} - \psi|^{1/2}\text{sign}(\hat{\psi} - \psi) + \mu_2(\hat{\psi} - \psi) \\ \phi_2(\hat{\psi} - \psi) = \frac{1}{2}\mu_1^2\text{sign}(\hat{\psi} - \psi) + \frac{3}{2}\mu_1\mu_2|\hat{\psi} - \psi|^{1/2}\text{sign}(\hat{\psi} - \psi) + \mu_2^2(\hat{\psi} - \psi) \end{cases}$

where $\mu_1 > 0$, $\mu_2 > 0$. The observer (26) is independent of the process kinetics and the tuning variables κ_1 , κ_2 , λ_ψ , μ_1 , and μ_2 are usually selected through a trial-and-error method. Comments can be drawn as follows: setting $\mu_1 = 0$ and $\mu_2 > 0$, (26) becomes a linear Luenberger observer, which can asymptotically estimate the true value only when S_{in} is constant. For varying inputs of substrate concentration, the estimation error of the linear observer is proportional to the size of the derivative and inversely proportional to the

observer gains. The observer (26) could achieve finite-time convergence for an arbitrary S_{in} with bounded derivatives. The relative gain values suggested by Levant [35] are $\kappa_1 = 2.2$ and $\kappa_2 = 1.5$, which should be chosen to obtain good convergence with the GSTO algorithm. Finally, λ_ψ affects both the convergence velocity and insensitivity to the change in S_{in} , as well as measurement noise.

3.2.2. Estimation of the Un-Measurable Biomass Concentration

To calculate ψ as well as the control (14) and (17), the biomass content X is needed besides the information of S and P . X is rendered difficult to measure on-line, and OBE is performed. Considering ethanol is the primary metabolite that is closely related to the content of biomass, X could be estimated through the construction of the observer on P . The procedure begins with the linearization of the subsystem in (1),

$$\begin{cases} \frac{dX}{dt} = -D|_{S_0, X_0, P_0} X + r_1|_{\mu_{m0}, S_0, P_0} \\ \frac{dP}{dt} = -D|_{S_0, X_0, P_0} P + r_2|_{S_0, P_0} \end{cases} \quad (27)$$

When (27) is non-singular, and D satisfies the persistent exciting (PE) condition, the non-biased estimation of P drives X to stably converge to the real value [36]. In the following, a Luenberger observer is constructed for P ,

$$\frac{d\widehat{P}}{dt} = -DP + \frac{r_1}{X} \cdot \widehat{X} + \omega_1(P - \widehat{P}) \quad (28)$$

where the hat represents the estimated value, and ω_1 is the observer coefficient. For the estimated P to converge to the measured one, the right-hand side of Equation (28) needs to approach zero, and the variation form gives an estimation of X ,

$$\frac{d\widehat{X}}{dt} = \gamma_1(P - \widehat{P}) / \left(\frac{r_2}{P} \right) \quad (29)$$

where γ_1 is a positive tuning parameter. Combining (28) and (29), the OBE on biomass concentration is formulated.

3.2.3. Estimation of the Fermentation Kinetics

As it can be seen, the specific reaction rate r_1 is involved for the aforementioned control and estimation, hence, estimation is performed in this section. Similar to the previous section, the OBE on r_1 is obtained using the on-line measurement of substrate concentration.

$$\frac{d\widehat{S}}{dt} = D(\widehat{S}_{in} - S) - \left(\frac{\widehat{r}_1}{Y_{SX}} + \frac{r_2}{Y_{SP}} \right) + \omega_2(S - \widehat{S}) \quad (30)$$

where ω_2 is another observer coefficient. And the estimator is given by,

$$\frac{d\widehat{r}_1}{dt} = - \left(\frac{\widehat{r}_1}{Y_{SX}} \right) / \left(\frac{r_2}{P} \right) \gamma_2(S - \widehat{S}) \quad (31)$$

where γ_2 is another positive tuning parameter.

The same procedure is conducted for the estimation of r_{O2} with the aid of on-line detection on dissolved oxygen O_2 ,

$$\begin{cases} \frac{d\widehat{O}_2}{dt} = K_L a_0 \cdot 1.024^{(T_r - 20)} (O_2^{sat} - O_2) - \widehat{r}_{O2} - DO_2 + \omega_3(O_2 - \widehat{O}_2) \\ \frac{d\widehat{r}_{O2}}{dt} = \gamma_3(O_2 - \widehat{O}_2) \end{cases} \quad (32)$$

where ω_3 and γ_3 are positive tuning parameters. Note that the estimated r_{O2} is able to accomplish the temperature control law (14).

The schematic of the nonlinear control stat from batch mode production is shown in Figure 4. The control system contains two coupling loops, and the control laws are (14) and (17), respectively. For the temperature control, we assume the modeling is precise and the regulator adopts exact linearizing control as the backbone and the unknown or varying parameters are obtained using the techniques of OBE and GSTO. For the control substrate concentration, the nonlinear GSC technique is formulated and batch and washout avoidance are embedded.

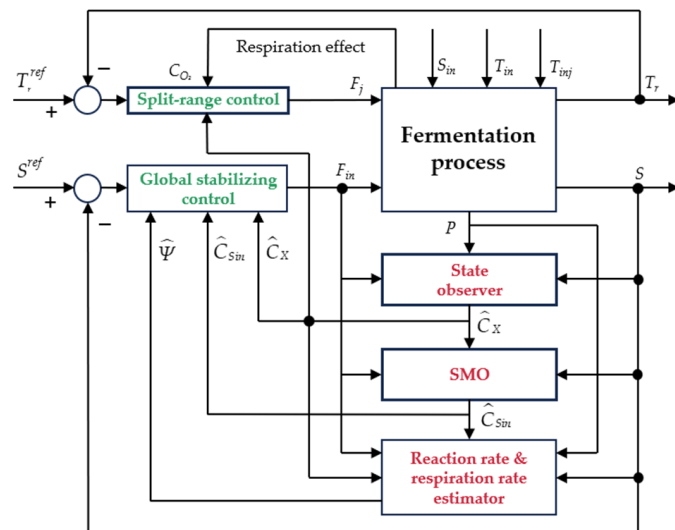


Figure 4. Structure of the coupled control loops for ethanol fermentation.

4. Results and Discussion

In this section, fermentation that starts from batch mode is controlled with the expectation to prolong the production period, avoid process instability, and assure a substantial production of ethanol and a minimal quantity of residual substrate, meanwhile regulating the temperature inside the bioreactor at suitable values. We start from investigation on suitable mathematical models that describe the complex kinetics. Furthermore, since the fermentation process is an exothermic one, detailed regression to characterize heat balance is essential for the control system. Then, controls in the perfect model, as well as a possible process–model mismatch by introducing field data, are tested and discussed.

4.1. Fermentation Modeling Issues

Here, we introduce a benchmark example with complete known kinetics to investigate relations of the states against S_{in} , which together with their measurement units are presented in Table 1 [37],

$$\begin{cases} \frac{dS}{dt} = D(S_{in} - S) - \left(\frac{\mu_m S / Y_{SX}}{S + K_s} \cdot e^{-K_E P} + \frac{\mu_p S / Y_{SP}}{S + K_{s1}} \cdot e^{-K_{E1} P} \right) X \\ \frac{dX}{dt} = -DX + r_1(S, X, P) = -DX + \frac{\mu_m S}{S + K_s} \cdot e^{-K_E P} X \\ \frac{dP}{dt} = -DP + r_2(S, X, P) = -DP + \frac{\mu_p S}{S + K_{s1}} \cdot e^{-K_{E1} P} X \end{cases} \quad (33)$$

However, considering the benchmark case is mainly applied for a scenario of continuous production, we regressed the kinetics (under 30 °C) using batch experiment data [37], and the updated parameters are listed Table 1. To regress the reaction kinetics, the mass conservation relation is revealed by Y_{SX} and Y_{SP} , which are obtained by fitting batch data; the kinetic parameters μ_m , K_s , and K_i are estimated using least squares regression of the integrated system (ode45 subroutine with the unknown parameters as the handle) against the field data, and the results are shown in Figure 5. Moreover, the empirical correlation of O_2^{sat} with varying T_r in Equation (3) is fitted under pH = 6 and represented as $f(T_r) = 14.16 - 0.39T_r + 0.00772T_r^2 + 0.000064T_r^3$ [38].

Table 1. Process and kinetic parameters—description and values [38].

Label	Description	Value	Label	Description	Value
A_1	Exponential factors in Arrhenius law	1.57×10^9	M_{Ca}	Mol mass of Ca	40 g/mol
A_2	Exponential factors in Arrhenius law	4.20×10^{33}	M_{Mg}	Mol mass of Mg	24 g/mol
A_T	Heat transfer area	1 m^2	M_{Cl}	Mol mass of Cl	35.5 g/mol
$C_{heat,r}$	Heat capacity of culture medium	$4.18 \text{ J/g/}^\circ\text{C}$	M_{CO_3}	Mol mass of CO_3	60 g/mol
$C_{heat,j}$	Heat capacity of the cooling agent	$4.18 \text{ J/g/}^\circ\text{C}$	M_{NaCl}	Mol mass of NaCl	58.5 g/mol
E_{a1}	Activation energy	$55,000 \text{ J/mol}$	M_{CaCO_3}	Mol mass of NaCO_3	100 g/mol
E_{a2}	Activation energy	$220,000 \text{ J/mol}$	M_{MgCl_2}	Mol mass of NaMgCl_2	95.2 g/mol
H_{OH}	Specific ionic constant of OH	0.941	R	Universal gas constant	$8.31 \text{ J/mol/}^\circ\text{C}$
H_H	Specific ionic constant of H	-0.774	Y_{SP}	Ethanol produced yield	0.3989 g/g
H_{CO_3}	Specific ionic constant of HCO_3	0.485	Y_{SX}	Biomass produced yield	0.607 g/g
H_{Cl}	Specific ionic constant of Cl	0.844	V	Bioreactor volume	1000 L
H_{Mg}	Specific ionic constant of Mg	-0.314	V_j	Cooling jacket volume	50 L
H_{Ca}	Specific ionic constant of Ca	-0.303	Y_{O_2}	O_2 consumed rate	0.970 mg/mg
H_{Na}	Specific ionic constant of Na	-0.55	ΔH_r	Aspiration heat	518 kJ/mol
I_i	Ionic strengths	-	μ_{O_2}	O_2 consumption rate	0.5 h^{-1}
K_{La0}	O_2 mass-transfer coefficient	38 h^{-1}	μ_P	Ethanol production rate	1.79 h^{-1}
K_{O_2}	O_2 consumption constant	8.886 mg/L	ρ_j	Density of jacket liquid	1000 g/L
K_E	Inhibition constant by ethanol	0.139 g/L	ρ_r	Density of the medium	1080 g/L
K_{E1}	Inhibition constant by ethanol	0.07 g/L	m_{NaCl}	Quantity of NaCl	500 g
K_S	Substrate constant for growth	1.03 g/L	m_{CaCO_3}	Quantity of CaCO_3	100 g
K_{S1}	Substrate constant for production	1.68 g/L	m_{MgCl_2}	Quantity of MgCl_2	100 g
K_T	Heat transfer coefficient	$3.6 \times 10^5 \text{ J/h/m}^2/\text{ }^\circ\text{C}$	M_{Na}	Molecular mass of Na	23 g/mol

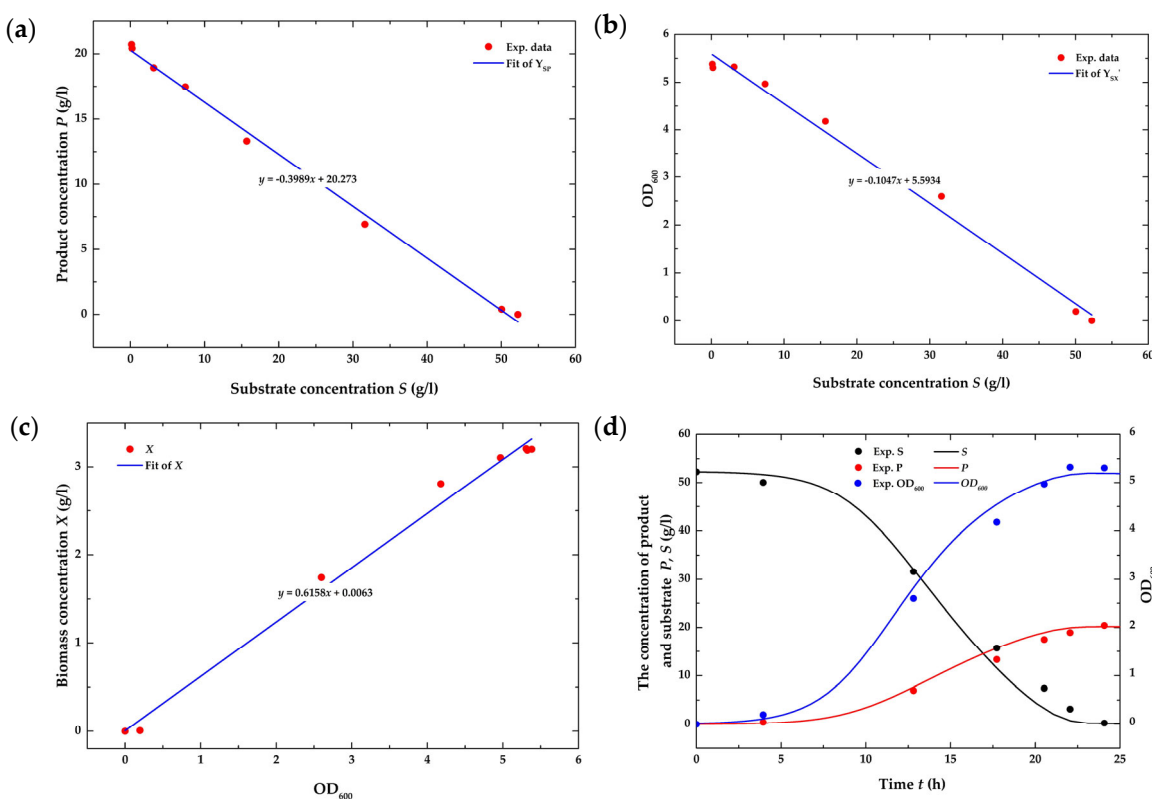


Figure 5. Experimental validation of the batch ethanol fermentation process. (a) Regression of Y_{SP} (0.3989) by experimental data of substrate concentration against the product ethanol; (b) Regression of Y_{SX} (0.105) by experimental data of substrate concentration against OD_{600} ; (c) Proportional relation of OD_{600} with the calculated biomass content, where the initial biomass is set as 0.01 by corrected inoculum size, and the biomass concentration is computed using literature data; (d) Fitting of the kinetics of Equation (33) using batch fermentation data.

4.2. Analysis of the Open-Loop System

Before conducting quantitative analysis, the general system (1) is revisited for a glimpse of the open-loop system stability. For a given initial condition (S_0, X_0, P_0) , Equation (1) is well-posed and, since $S(t \rightarrow +\infty) \leq S_{in} < +\infty$, $P(t \rightarrow +\infty) \leq (1/Y_{SP} + \beta/Y_{SX})S_{in} < +\infty$, and $r_2(., P)$ decreases with the increase in P , all non-negative set $\Omega = \{(S, X, P) : \geq 0\}$ values lie in the bounded set Ω eventually as time approaches infinity, indicating that the unlimited duplication of cells or sustained accumulation of ethanol is not possible. Note that output multiplicity exists for this system, where, apart from the trivial solution $(S_{in}, 0, 0)$, we represent the non-trivial one as (S^*, X^*, P^*) , and the global stability property is provided by the following Theorem 2.

Theorem 2. Assume $r_1/r_2 = \beta$ is a constant, the stability criterion provides $D_c < D$, the travail solution $(S_{in}, 0, 0)$ is asymptotically stable; $D_c > D$, the non-travail solution (S^*, X^*, P^*) is asymptotically stable; $D_c = D$, both solutions are coincident and a branch point (BP) emerges, where $D_c = r_1(S_{in}, P)/X^*$.

Proof. With a high-substrate environment and to avoid ethanol inhibition, β is viewed as a constant, X and P share identical dynamics, and (1) is reduced to second order. The equilibrium of the reduction system presents output multiplicity, and besides the travail solution $(S_{in}, 0, 0)$, the non-trivial one gives,

$$S^* = D \cdot \frac{S^* + K_s}{\mu_m} \cdot e^{K_E P^*}; P^* = (S_{in} - S^*) / \left(\frac{\beta}{Y_{SX}} + \frac{1}{Y_{SP}} \right); X^* = \beta P^*. \quad (34)$$

As for the exploration of asymptotic behavior, we first implement dimensional reduction analysis. Laplace transform of the second and third formula in (1) gives,

$$L \begin{pmatrix} \frac{dX}{dt} = -DX + r_1 \\ \frac{dP}{dt} = -DP + r_2 \end{pmatrix} = \frac{sX = -DX + r_1}{sP = -DP + r_2} \Rightarrow \frac{X(s)}{P(s)} = \beta \quad (35)$$

which indicates that $P(t)$ and $X(t)$ share identical dynamic trajectories, and for any casually assigned initial states (X_0, P_0) , the ethanol accumulation rate is proportional to the increase in yeast. Then, the characteristic equation of the limited system $[S, X]$ provides,

$$\left[\lambda / \left(\frac{\beta}{Y_{SX}} + \frac{1}{Y_{SP}} \right) + D \right] (D + \lambda - \mu) = 0 \quad (36)$$

Since $\lambda_1 = -D \times (\beta/Y_{SX} + 1/Y_{SP})$ is negative, local stability is determined by $\lambda_2 = \mu - D$, where $\mu(S, P)$ decreases with the increase of P because of the inhibitory effect. Moreover, the asymptotic property of the limiting system provides,

$$\begin{cases} \frac{dX}{dt} = \left(\mu \left(S_{in} - \left(\frac{\beta}{Y_{SX}} + \frac{1}{Y_{SP}} \right) P \right) f(P) - D \right) X = (F_2(P) - D) X \\ \frac{dP}{dt} = \frac{\rho}{\mu} \mu \left(S_{in} - \left(\frac{\beta}{Y_{SX}} + \frac{1}{Y_{SP}} \right) P \right) f(P) X - DP = F_1(P) X - DP. \end{cases} \quad (37)$$

where $f(P)$ is the product-inhibition term. Then, $F_i(P) = \mu(S_{in} - (\beta/Y_{SX} + 1/Y_{SP})P)f(P)$ for $i = 1, 2$. Hence, $F_i(0) = \mu(S_{in})$, $F_i((\beta/Y_{SX} + 1/Y_{SP})S_{in}) = 0$, and $F_i'(P) \leq 0$ if $0 \leq P \leq (\beta/Y_{SX} + 1/Y_{SP})S_{in}$. The vector form gives,

$$Y' = F(Y), Y(0) = Y_0. \quad (38)$$

when $D_c = \mu(S_{in}, P = 0) \leq D$, $(0,0)$ is the only equilibrium and it is locally stable; when $D_c > D$, $(X^*, P^*) = (DF_2^{-1}(D)/F_1(F_2^{-1}(D)), F_2^{-1}(D))$ is locally stable and $(0, 0)$ becomes unstable.

When $D = D_c$, (X^*, P^*) degenerates to the washout condition. Substituting $F(P)$ to system (24), one has,

$$\begin{aligned} \left(\frac{1}{X}F\right) &= \frac{\partial}{\partial X}(F_1(P) - D) + \frac{\partial}{\partial P}(F_2(P) - \frac{DP}{X}) \\ &= F'(P) - \frac{D}{X} < 0 \end{aligned} \quad (39)$$

By the Poincare–Bendixson theorem, the equilibrium is globally stable. \square

In the following, process states with varying parameters D and S_{in} are analyzed. Although process–model mismatch is inevitable, quantitative analysis undertaken with fully known kinetics is essential because certain guidelines could be provided to aid in finding out optimal working conditions. As is shown in Figure 6, with the increase in D , P decreases rapidly till approaching zero, and the washout condition emerges and is labeled as BP, where all substrate is left unconsumed. For a given D , increasing S_{in} results in a limited effect on production P in the low D region, but the curves coincide at the high D region, which indicates that extra substrate supply is not constructive for process enhancement (Figure 6b). Moreover, the emergence of the washout condition is insensitive with varying S_{in} . Further plots of (S_{in}, S) and (S_{in}, P) reveal that the identical slope k exists when the substrate content is adequate, which means ΔS^* is proportional to deviation of S_{in} , and from Equation (33) we have,

$$(1 - k)\Delta S_{in} = \left(\frac{\beta}{Y_{SX}} + \frac{1}{Y_{SP}}\right)\Delta(\delta P) \quad (40)$$

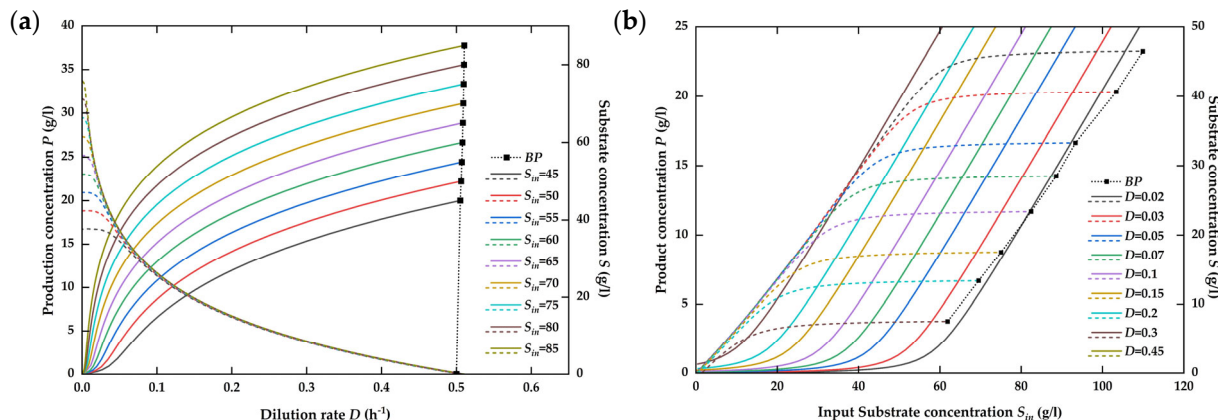


Figure 6. Numerical continuation of the ethanol fermentation process with varying parameters. (a) Ethanol production under varying dilution rate and input substrate concentration; (b) Influence of input substrate concentration on fermentation rate.

Since the limiting substrate is expected to be adequate in continuous fermentation, the (D, P) plots are identical with varying S_{in} , then, $\Delta(\delta P) = 0$ and $k = 1$. In Equation (40), which indicates regulating substrate S^{ref} under a chemostat by law (17) and regulating the cell number X^{ref} using turbidostats in Remark 5, there are dual problems [39] so long as washout avoidance [40] conditions are promised.

To avoid washout, cell duplication should exceed cell loss, and the upper bound of D is provided as follows,

$$\lim_{X \rightarrow 0^+} \frac{r_1(0, S, \cdot)}{X} - D > \varepsilon \quad (41)$$

where $\varepsilon \geq 0$ is the minimal allowable cell accumulation rate. To mention, ε is difficult to quantify in real applications. Hence, we provide to start the control from batch fermentation and GCS is implemented to promise shifting from a batch model to a continuous one. With the control law (17), D is unprovoked at the beginning and lasts for a while under very small initial $\gamma_0 = \gamma(t_0 = 0)$, and the influence of varying S_{in} during this interval is avoided.

To mention, the control starting by traditional batch mode production is easily applicable in practice, and after the cell is substantially accumulated, CER becomes detectable and $r_1 > 0$ makes the actuator functional; then, with the bounded co-state γ , the control can track any reference $S^{ref} < S_{in}$, even it is unreachable.

However, the above-mentioned control is conducted on a casually assigned S^{ref} , where extra substrate would not increase ethanol production once the supply is adequate; hence, a well-prescribed reference trajectory is crucial, especially when S_{in} is time-varying and productivity increase is one of the main purposes. From Figure 6a, the chemostat method expects the depletion of substrate to increase feed conversion and downsize subsequent ethanol separation/purification burden, but the unlimited decrease of the dilution rate might not be a reasonable choice, since when D approaches zero, the process becomes batch mode. Moreover, the capability of cells to consume a trace quantity of substrate varies from stain to stain, and when the substrate is not adequate, ethanol productivity decreases rapidly. One can give the batch avoidance condition similar to Equation (41) to construct the lower bound D in the control system. On the condition that the substrate in the fermenter needs to exhibit a decreasing trend, i.e., assume the initial $S_0 > 0$, and without the interference of feed supply, $S(t)$ is repellent to S_0 ; then, the lower bound is provided,

$$\lim_{S \rightarrow 0^+} D - \frac{r_1(X, S, \cdot)}{X} > \varepsilon \quad (42)$$

Likewise, Equation (42) is difficult to apply in practice. Concerning this, any fermenter i in the series (Figure 3) is expected to work with adequate substrate to promise a high ethanol conversion rate, and $k = 1$ in Equation (40) could be provided as the indicator to explore D in the lower bound that minimizes residual substrate. Hence, in this work, we formulate S^{ref} to maintain $k = 1$ for the deterministic system, and for the case of unknown metabolic capabilities, the ladder pattern S^{ref} is constructed as the reference trajectory and D in the lower bound is obtained by a trial-and-error method.

4.3. Numerical Simulation on the Closed-Loop System

In the present section, the behavior of OBE under the control prescribed in Figure 4 is compared with the simulation results of the perfect model with parameters provided in Table 1 (fermentation kinetics are validated). The process starts from batch mode, and the initial states $(S_0, X_0, P_0) = (52.64, 0.01, 0)$ g/L are verified against the experimental settings. Other operating conditions are the inlet substrate temperature $T_{in} = 25$ °C and the jacket cooling agent $T_{inj} = 15$ °C. Furthermore, T_{in} and T_{inj} are introduced with sinusoidal-like perturbations to mimic the influence of the feedback stream in Figure 2.

Temperature change in the fermenter is led by two factors: (1) the aerobic effect caused by the dissolved oxygen would lead to a gradual temperature increase; (2) the enthalpy deficit with the action of D might lead to rapid temperature decline. Therefore, we formulate the split-ranging control exhibited in Figure 7 to regulate the temperature inside the bioreactor. We set ΔH_m as the phase changing heat for per kg steam, and if roughly taking $\alpha = \Delta H_m / C_{heat,j} / (T_{inj} - T_j)$ as a constant, say 5.0 in the current case, a control simulation can be implemented under the unified control law (14). F_j being negative indicates steam being injected to the jacket, while positive means cooling water is used. We assume F_j is bounded with $[-1000, 2000]$ L/h, where negative values indicate the "B" valve is open and positive values mean the "A" valve is in operation.

Since the fermenter volume V is much bigger than the jacket volume V_j , the response of the manipulated variable is slow, and hysteresis led by inertia is expected to be compensated by actions ahead of time. Therefore, PD control is integrated to (14) to account for the change in T_r ,

$$F_j(t) = \frac{\rho_r C_{heat,r}}{\rho_j C_{heat,j}} \frac{V}{T_{inj} - T_j} \left(\eta \left(\left(k + T_d \frac{N}{1 + N/s} \right) (T_r^{ref} - T_r) \right) - \frac{\Delta H_r r_{O_2}}{32 \rho_r C_{heat,r}} - D(T_{in} - T_r) \right) \quad (43)$$

where k represents the gain, T_d is the differential time, and N is the filter constant. Because the response of fermentation states is slower than that of temperature, fine-tuned temperature control is exploited first, and we expect T_r is well-controlled so as to alleviate interference between loops.

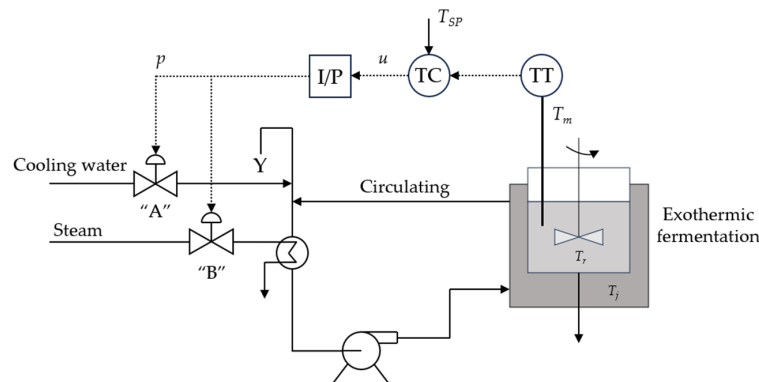


Figure 7. The split-ranging control schematic. When the actuators are off, “A” is in operation to remove the extra heat, and when the discharge/refill valves are open, “B” is in operation to remit the enthalpy loss.

The behavior of the closed-loop system adopting the adaptive law (43) under the specific $F_{in} = 26 \text{ g/L}$ is shown in Figure 8. The graphics in Figure 8a–c represent the behavior of the estimation variables X , r_{O2} , and S_{in} , while the graphic plotted in Figure 8d is related to the control input F_j and response T_r . For the estimation of biomass concentration, P is assumed to be on-line measurable, and during the observation of P , OBE is implemented to obtain an estimation of X ; hence, the estimation of P (P^* in Figure 8a) is convergent to the real value faster than that of X . Similarly, oxygen demand is detected on-line which is used for estimation of r_{O2} , but the aspiration effect is also influenced by biomass content; therefore, in Figure 8b, the estimation effect of r_{O2} is also affected by X^* in Figure 8a.

The estimation of the input substrate concentration is more difficult because no direct one-on-one detectable signal could be mapped on S_{in} , and we introduce an extra variable ψ defined in Equation (24) to represent S_{in} . The underlying idea follows principle of substrate conservation; hence, for the detection of ψ , all three fermentation related states (S , X , P) are required, from measurement instruments or by estimation. When the estimation of ψ tracks the real value well, OBE could be adopted to estimate S_{in} . In this work, a second-order SMO by the technique of GSTO is proposed for the estimation of S_{in} , and the tracking effect is provided in Figure 8c, and one can expect that the higher-order SMO tracks the real value better; however, the tuning parameters also increase.

Figure 8d presents the result of temperature control using the adaptive regulator (43), where the estimation of r_{O2} is essential because the respiration effect is one of the main sources for temperature increase; note that an estimation of r_{O2} is provided in Figure 8b through the observation of X . The trajectory for F_j reveals that steam is supplied at the beginning to warm up the fermentation process, and with the duplication cells, oxygen consumption leads the split-range control to gradually close the steam valve, then open up the cooling water. Compared to Figure 8a–c, we can infer that temperature inputs/states have limited influence on fermentation temperature; moreover, the feed-forward effect of (43) is revealed by a longer duration of settling in the time for F_j than for T_r .

First case scenario. In this scenario, the set-points of the two controlled variables were fixed at two constant values, respectively, $S^{ref} = 60 \text{ g/L}$ and $T_r^{ref} = 30.0 \text{ }^\circ\text{C}$. By analyzing Figure 9a,b, it results that the proper domain $\gamma \in (\gamma_m, \gamma_M)$ promises anti-saturation of the control F_{in} . As in this case, S^{ref} is higher than the initial $S_0 = 56.2 \text{ g/L}$ starting from batch mode production, γ reaches γ_M and keeps the maximum value, whilst F_{in} decreases gradually after a quick supplement of substrate at the beginning, though the deviation $S^{ref} - S$ always exists. Hence, the control could avoid input saturation; moreover, the

fermentation process could shift from batch mode to a continuous one with an increase trend in ethanol production.

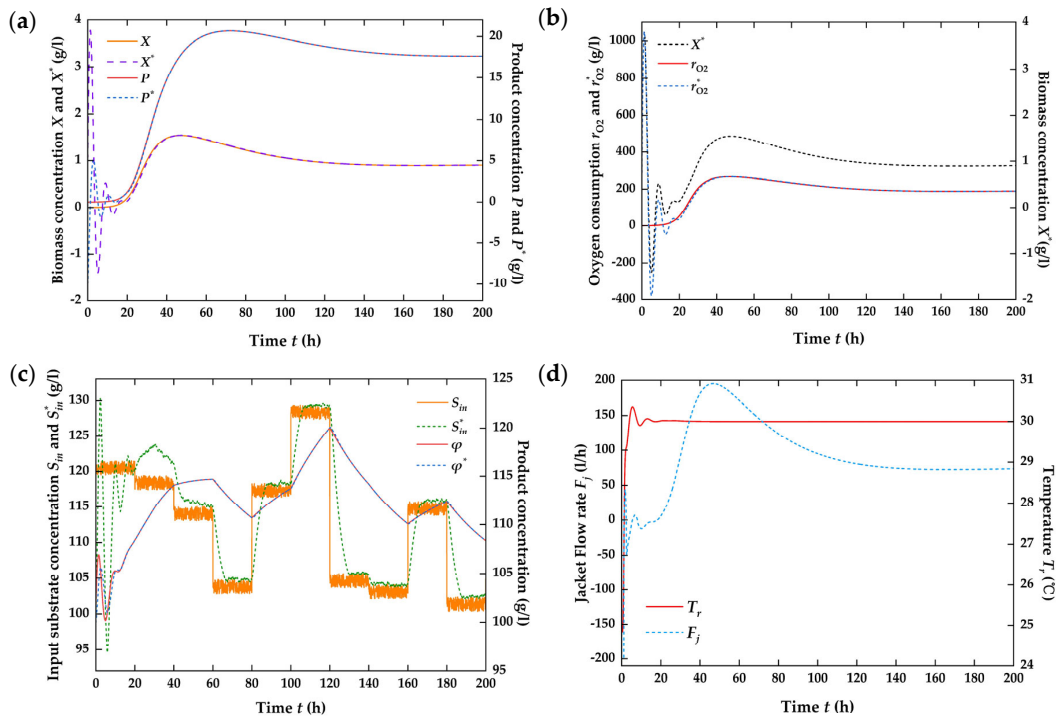


Figure 8. State estimation and temperature control through control law (43) with constant $F_{in} = 26 \text{ l/h}$.
(a) Estimation of X by observation of P , where $\omega_1 = 0.5$ and $\gamma_1 = 0.75$. **(b)** Estimation of r_{O2} by observation of X , where $\omega_3 = 0.5$ and $\gamma_3 = 1.0$. **(c)** Estimation of S_{in} by 2nd order SMO of ψ , where $\kappa_1 = 0.075$, $\kappa_2 = 2.5$, $\lambda_\psi = 2.5$, $\lambda_{\psi 1} = 2.5$, $\omega_2 = -1$, $\mu_1 = 3.8$, $\mu_2 = 2.1$, $\gamma_3 = 1.0$. **(d)** | $K_P = 0.5$, $K_I = 0$, $K_D = 1.5$, $\eta_2 = 0.5$.

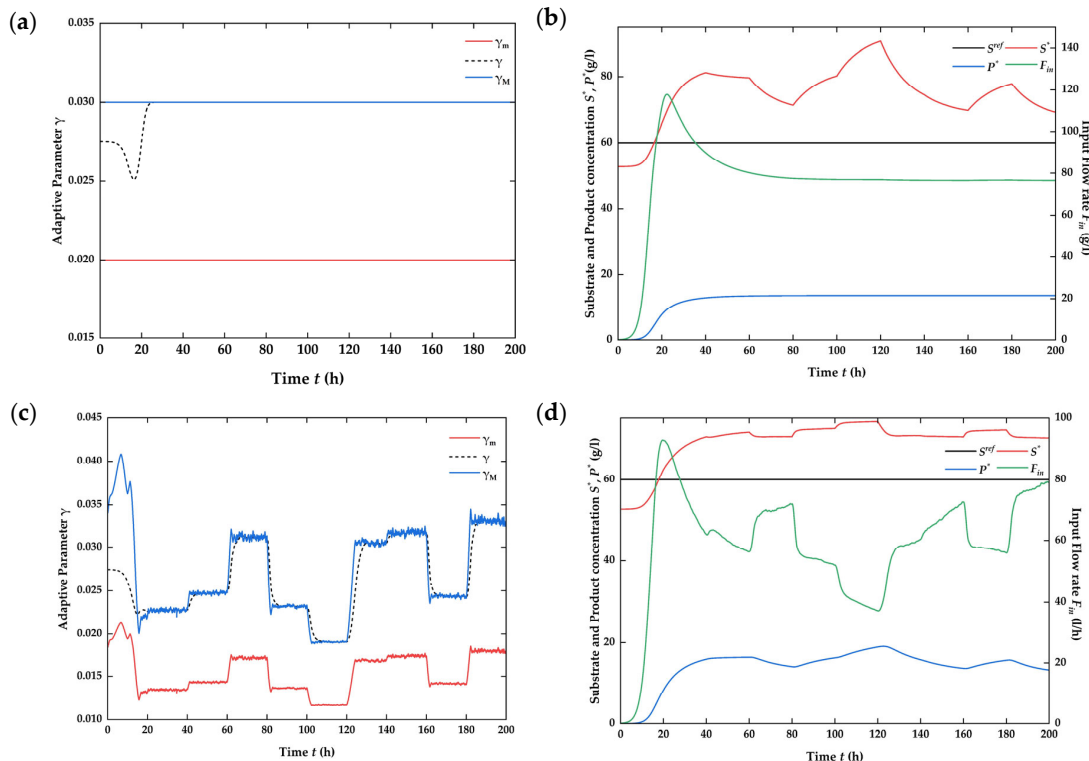


Figure 9. Cont.

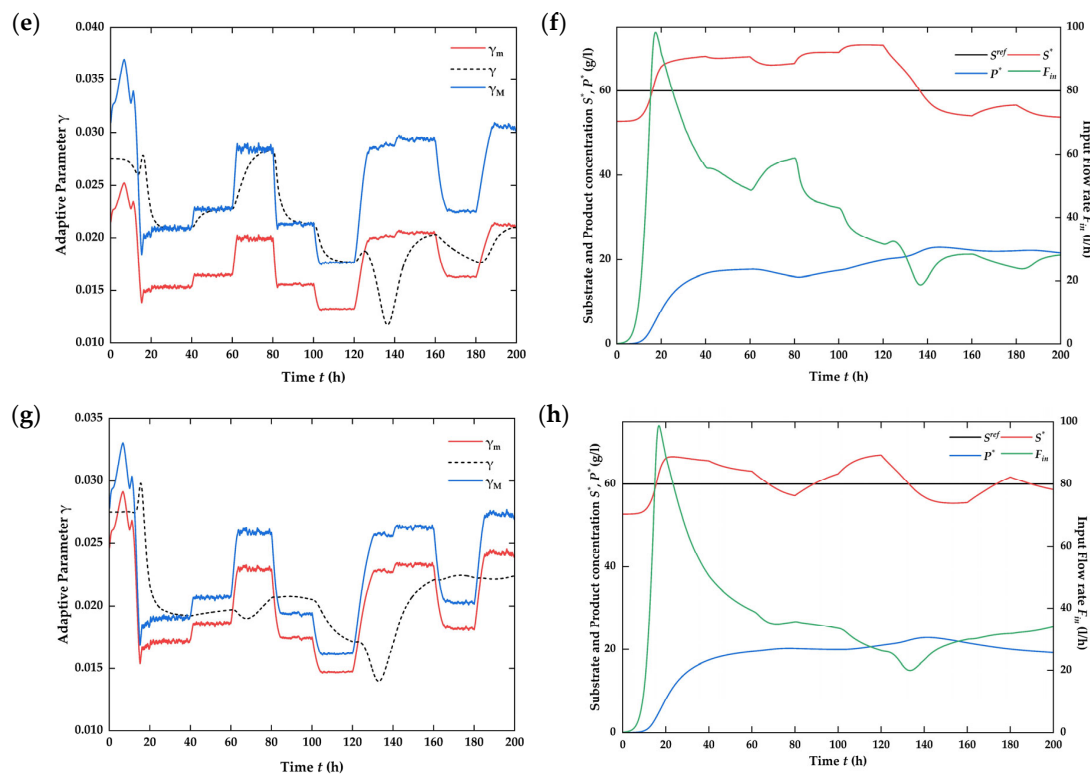


Figure 9. Global stabilizing control through (17) with estimation, where $S^{ref} = 60 \text{ g/L}$ and $T_r^{ref} = 30.0^\circ\text{C}$. (a) Adaptive control with fixed parameters $\gamma_m = 0.02$ and $\gamma_M = 0.03$. (b) Control performance under $K = 2.5$ and fermenter states. (c) Control with adaptive parameters $(\gamma_m, \gamma_M) = \gamma^{ref} \pm 0.5 \times S(\gamma^{ref}/S_{in})$. (d) Control performance under $K = 2.5$ and fermenter states. (e) Control with adaptive parameters $(\gamma_m, \gamma_M) = \gamma^{ref} \pm 0.3 \times S(\gamma^{ref}/S_{in})$. (f) Control performance under $K = 2.5$ and fermenter states. (g) Control with adaptive parameters $(\gamma_m, \gamma_M) = \gamma^{ref} \pm 0.1 \times S(\gamma^{ref}/S_{in})$. (h) Control performance under $K = 2.5$ and fermenter states.

In the following, we consider the practical case that γ_m and γ_M are time-varying when inputs vary. As is shown in Figure 9c,d, γ_m and γ_M follow the trend of S_{in} estimation and when the scope between (γ_m, γ_M) is set as $S(\gamma^{ref}/S_{in})$, γ reaches γ_M and follows the trend (Figure 9c), and results in S to increase and maintain a high substrate run-off (Figure 9d). We can narrow down the regime (γ_m, γ_M) to force $S \rightarrow S^{ref}$: Figure 9e,g are the adaptive parameters under 0.6 and 0.2 times $S(\gamma^{ref}/S_{in})$, respectively, and the corresponding control results are shown in Figure 9f,h. The control becomes aggressive when the domain of γ narrows down. Note that the fermentation reaction is very slow, and it is probable that the delay in response to the broth changes might deteriorate the control performance in real-time practice; hence, our purpose is not to precisely maintain the values at their reference but to shift between different operation modes with the least possible substrate loss.

Second case scenario. To increase ethanol conversion and decrease substrate loss, the second scenario is carried out considering that the reference S^{ref} has a decreasing evolution under piece-wise constant steps, where the domains of the adaptive parameters (γ_m, γ_M) are set as 0.2 times $S(\gamma^{ref}/S_{in})$. As is shown in Figure 10a, the reference jumps at $t = 50 \text{ h}$, 15 h , and 300 h directly correspond to the scope change in γ_m and γ_M ; however, the adaptive law promises γ to vary continuously, which is advantageous for system sensitive to external interference.

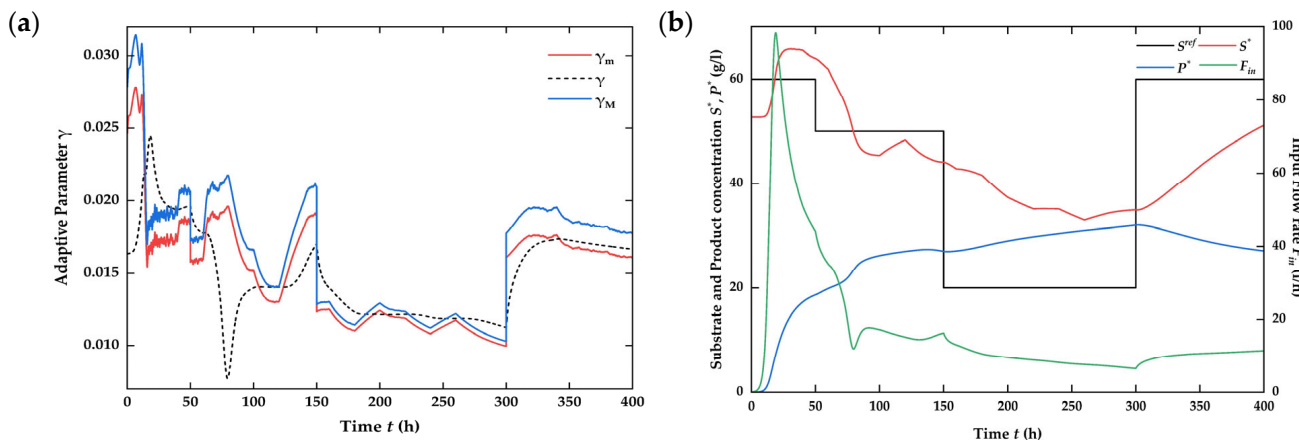


Figure 10. Global stabilizing control with ladder form reference tracking, where $S^{ref} = 60$ g/L and $T_r^{ref} = 30.0$ °C. (a) Adaptive control with fixed parameters $\gamma_m = \gamma^{ref} - S(\gamma^{ref}/S_{in})$ and $\gamma_M = \gamma^{ref} + S(\gamma^{ref}/S_{in})$. (b) Control performance under $K = 2.5$ and fermenter states.

One problem related to the economically viable control is the selection of optimal reference S^{ref} . To make the system continuous and functional, batch/washout avoidance is essential; hence, we wish the control input F_{in} to be somewhat inert to changes. As is shown in Figure 10b, for the ladder form decrease of S^{ref} at $t \in (0, 300)$ h, F_{in} tends to decrease after a quick increase at the beginning. Though $S^{ref} = 20$ g/L is hard to reach, ethanol production continues to increase. Here, we can expect an optimal S in this case of around 30 g/L, and the corresponding F_{in} decrease to about 11 L/h. Further increase $S^{ref} = 60$ g/L and the results show that ethanol production decreases and F_{in} increases slowly, indicating that the adaptive control is capable of maintaining continuous production whilst keeping F_{in} at a low flowrate, so as to decrease substrate loss. To mention, the process shift from batch mode to continuous mode is critical for the fermentation process, and we have noticed a time during exists before the start-up operation in dilution rate, which allows for cell accumulation, and during this time interval, the system is in batch mode. In the following, we introduce experimental collected CER signals and tests on this control system to evaluate the start-up procedure.

4.4. Assessment of Process Improvement [41]

To appreciate how the implementation of the continuous strategy could potentially impact ethanol production goals over a long-term period, we compared the results of Figure 9g,h with a batch in terms of ethanol productivity, substrate conversion, and substrate loss. For a reactor with a working volume (V) of 10^5 L, the downtime between batches was estimated at 6.0 h and the batch results repeated the regression of Figure 5d, as is exhibited in Figure 11a. The simulation results in a ~200 h interval show that the averaged ethanol productivity for continuous fermentation reaches 0.669 g L $^{-1}$ h $^{-1}$, which is 19.7% higher than the batch mode with the same start-up condition.

To evaluate substrate utility, the substrate conversion ratio (dP/dS) and substrate loss are presented in Figure 11a; the average conversion ratio in continuous mode is 0.369, while batch mode could be $Y_{SP} = 0.3989$ because the substrate loss of batch fermentation is very small. However, the substrate loss of continuous fermentation is substantial, for the current case where S^{ref} is set as 60 g/L, the average outlet reaches 60.78 g/L. To mention, the configuration exhibited in Figure 3 is an effective solution to enhance substrate utility.

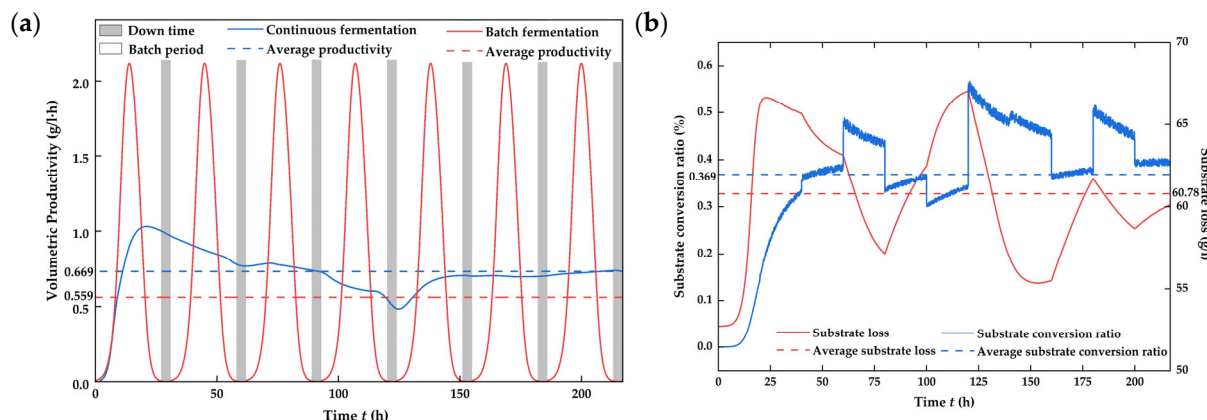


Figure 11. Comparison of batch and continuous fermentation with the same start-up condition for 200 h interval. (a) Volumetric productivity for batch and continuous fermentation. (b) Substrate conversion ratio and substrate loss of the continuous mode.

5. Conclusions

In this paper, a mathematical model for ethanol fermentation is proposed and validated with experimental data. Then, an innovative global stabilizing control scheme is developed and applied for continuous ethanol production that is started from batch mode. To address the problem of fermentation state monitoring, observer-based estimation strategies are developed, and for the estimation of unknown inputs, the technique of a higher-order sliding mode observer is adopted. Despite being in harsh, realistic operating conditions (unknown input substrate concentration, time-varying and uncertain kinetics, noisy measurements), the adaptive control structure behaved well, and the control achieves a 19.7% increase in volumetric productivity. The reported simulation results are encouraging, and the proposed control structure can be adapted to other types of fermentation processes.

Author Contributions: All authors contributed to the study conception and design. Material preparation, data collection, and analysis were performed by Y.Q. and C.Z. The first draft of the manuscript was written by Y.Q., and both authors commented on previous versions of the manuscript. All authors have read and agreed to the published version of the manuscript.

Funding: The authors gratefully acknowledge the following institutions for their support: Yunnan Major Scientific and Technological Projects (Grant No. 202202AG050001); Yunnan basic research project (Grant No. 202001AU070048).

Data Availability Statement: All data generated or analyzed during this study are included in this published article.

Conflicts of Interest: The authors declare that they have no conflicts of interest.

References

- Gonçalves, F.; Perna, R.; Lopes, E.; Maciel, R.; Tovar, L.; Lopes, M. Strategies to improve the environmental efficiency and the profitability of sugarcane mills. *Biomass Bioenerg.* **2021**, *148*, 106052. [[CrossRef](#)]
- Bilal, M.; Wang, Z.; Cui, J.D.; Ferreira, L.F.R.; Bharagava, R.N.; Iqbal, H.M.N. Environmental impact of lignocellulosic wastes and their effective exploitation as smart carriers—A drive towards greener and eco-friendlier biocatalytic systems. *Sci. Total Environ.* **2020**, *722*, 137903. [[CrossRef](#)] [[PubMed](#)]
- Deng, W.P.; Feng, Y.C.; Fu, J.; Guo, H.W.; Guo, Y.; Han, B.X.; Jiang, Z.C.; Liu, H.C.; Nguyen, P.T.T.; Ren, P.N.; et al. Catalytic conversion of lignocellulosic biomass into chemicals and fuels. *Green Energy Environ.* **2023**, *8*, 10–114. [[CrossRef](#)]
- Daugulis, A.J.; McLellan, P.J.; Li, J. Experimental investigation and modeling of oscillatory behavior in the continuous culture of *Zymomonas mobilis*. *Biotechnol. Bioeng.* **1997**, *56*, 99–105. [[CrossRef](#)]
- Herrera, W.E.; Rivera, E.C.; Alvarez, L.A.; Tovar, L.P.; Rojas, S.T.; Yamakawa, C.K.; Bonomi, A.; Maciel, R. Modeling and control of a continuous ethanol fermentation using a mixture of enzymatic hydrolysate and molasses from sugarcane. In Proceedings of the 2nd International Conference on Biomass, Taormina, Italy, 19–22 June 2016.

6. Quintero, O.L.; Amicarelli, A.A.; Scaglia, G.; di Sciascio, F. Control based on numerical methods and recursive Bayesian estimation in a continuous alcoholic fermentation process. *BioResources* **2009**, *4*, 1372–1395. [[CrossRef](#)]
7. Blanco-Sánchez, P.; Taylor, D.; Cooper, S. IEA Bioenergy Task 33 UK Country Report; International Energy Agency Bioenergy: Paris, France, 2021.
8. Skupin, P.; Laszczyk, P.; Goud, E.C.; Vooradi, R.; Ambati, S.R. Robust nonlinear model predictive control of cascade of fermenters with recycle for efficient bioethanol production. *Comput. Chem. Eng.* **2022**, *160*, 107735. [[CrossRef](#)]
9. Das, S. Mathematical Modelling of Bioenergy Systems for Stability Analysis and Parametric Sensitivity. Ph.D. Thesis, UiT The Arctic University of Norway, Tromsø, Norway, 2021.
10. Zhai, C.; Yang, C.X.; Na, J. Bifurcation Control on the Un-Linearizable Dynamic System via Washout Filters. *Sensors* **2022**, *22*, 9334. [[CrossRef](#)] [[PubMed](#)]
11. Straathof, A.J.J. Modelling of end-product inhibition in fermentation. *Biochem. Eng. J.* **2023**, *191*, 108796. [[CrossRef](#)]
12. Kurth, J.M.; Nobu, M.K.; Tamaki, H.; de Jonge, N.; Berger, S.; Jetten, M.S.M.; Yamamoto, K.; Mayumi, D.; Sakata, S.; Bai, L.P.; et al. Methanogenic archaea use a bacteria-like methyltransferase system to demethoxylate aromatic compounds. *ISME J.* **2021**, *15*, 3549–3565. [[CrossRef](#)] [[PubMed](#)]
13. Tu, B.P.; Kudlicki, A.; Rowicka, M.; McKnight, S.L. Logic of the yeast metabolic cycle: Temporal compartmentalization of cellular processes. *Science* **2005**, *310*, 1152–1158. [[CrossRef](#)] [[PubMed](#)]
14. Sriputorn, B.; Laopaiboon, P.; Phukoetphim, N.; Polsokchuak, N.; Butkun, K.; Laopaiboon, L. Enhancement of ethanol production efficiency in repeated-batch fermentation from sweet sorghum stem juice: Effect of initial sugar, nitrogen and aeration. *Electron. J. Biotechnol.* **2020**, *46*, 55–64. [[CrossRef](#)]
15. Peng, P.; Lan, Y.; Liang, L.; Jia, L. Membranes for bioethanol production by pervaporation. *Biotechnol. Biofuels* **2021**, *14*, 10. [[CrossRef](#)] [[PubMed](#)]
16. Chai, W.Y.; Teo, K.T.K.; Tan, M.K.; Tham, H.J. Fermentation Process Control and Optimization. *Chem. Eng. Technol.* **2022**, *45*, 1731–1747. [[CrossRef](#)]
17. Chai, W.Y.; Teo, K.T.K.; Tan, M.K.; Tham, H.J. Model predictive control in fermentation process—A review. In Proceedings of the 2nd Energy Security and Chemical Engineering Congress, Gambang, Malaysia, 29 August 2022.
18. Shen, Y.; Zhao, X.Q.; Ge, X.M.; Bai, F.W. Metabolic flux and cell cycle analysis indicating new mechanism underlying process oscillation in continuous ethanol fermentation with *Saccharomyces cerevisiae* under VHG conditions. *Biotechnol. Adv.* **2009**, *27*, 1118–1123. [[CrossRef](#)] [[PubMed](#)]
19. Prasad, D.; Kumar, M.; Srivastav, A.; Singh, R.S. Modelling of Multiple Steady-state Behavior and Control of a Continuous Bioreactor. *Indian J. Sci. Technol.* **2019**, *12*, 140476. [[CrossRef](#)]
20. Bai, F.W.; Zhao, X.Q. High gravity ethanol fermentations and yeast tolerance. In *Microbial Stress Tolerance for Biofuels*; Springer: Berlin/Heidelberg, Germany, 2011.
21. Navarro-Tapia, E.; Nana, R.K.; Querol, A.; Pérez-Torrado, R. Ethanol cellular defense induce unfolded protein response in yeast. *Front. Microbiol.* **2016**, *7*, 189. [[CrossRef](#)] [[PubMed](#)]
22. Lopez, P.C.; Feldman, H.; Mauricio-Iglesias, M.; Junicke, H.; Huusom, J.K.; Gernaey, K.V. Benchmarking real-time monitoring strategies for ethanol production from lignocellulosic biomass. *Biomass Bioenerg.* **2019**, *127*, 105296.
23. Periyasamy, S.; Isabel, J.B.; Kavitha, S.; Karthik, V.; Mohamed, B.A.; Gizaw, D.G.; Sivashanmugam, P.; Aminabhavi, T.M. Recent advances in consolidated bioprocessing for conversion of lignocellulosic biomass into bioethanol—A review. *Chem. Eng. J.* **2022**, *453*, 139783. [[CrossRef](#)]
24. Petre, E.; Selișteanu, D.; Roman, M. Advanced nonlinear control strategies for a fermentation bioreactor used for ethanol production. *Bioresour. Technol.* **2021**, *328*, 124836. [[CrossRef](#)] [[PubMed](#)]
25. Ciesielski, A.; Grzywacz, R. Nonlinear analysis of cybernetic model for aerobic growth of *Saccharomyces cerevisiae* in a continuous stirred tank bioreactor. Static bifurcations. *Biochem. Eng. J.* **2019**, *146*, 88–96. [[CrossRef](#)]
26. Perrier, M.; Dochain, D. Evaluation of control strategies for anaerobic digestion processes. *Int. J. Adapt. Control. Signal Process.* **1993**, *7*, 309–321. [[CrossRef](#)]
27. Czyżniewski, M.; Łangowski, R. A robust sliding mode observer for non-linear uncertain biochemical systems. *ISA Trans.* **2022**, *123*, 25–45. [[CrossRef](#)]
28. Petre, E.; Selișteanu, D.; Roman, M. Control schemes for a complex biorefinery plant for bioenergy and biobased products. *Bioresour. Technol.* **2020**, *295*, 122245. [[CrossRef](#)]
29. Pachauri, N.; Rani, A.; Singh, V. Bioreactor temperature control using modified fractional order IMC-PID for ethanol production. *Chem. Eng. Res. Des.* **2017**, *122*, 97–112. [[CrossRef](#)]
30. Pachauri, N.; Singh, V.; Rani, A. Two degrees-of-freedom fractional-order proportional–integral–derivative-based temperature control of fermentation process. *J. Dyn. Syst. Meas. Control.* **2018**, *140*, 071006. [[CrossRef](#)]
31. Sun, S.Y.; Gresham, D. Cellular quiescence in budding yeast. *Yeast* **2021**, *38*, 12–29. [[CrossRef](#)] [[PubMed](#)]
32. Oh, T.H.; Park, H.M.; Kim, J.W.; Lee, J.M. Integration of reinforcement learning and model predictive control to optimize semi-batch bioreactor. *AIChE J.* **2022**, *68*, e17658. [[CrossRef](#)]
33. Pinto, A.S.S.; Pereira, S.C.; Ribeiro, M.P.A.; Farinas, C.S. Monitoring of the cellulosic ethanol fermentation process by near-infrared spectroscopy. *Bioresour. Technol.* **2016**, *203*, 334–340. [[CrossRef](#)] [[PubMed](#)]

34. Tiernan, H.; Byrne, B.; Kazarian, S.G. ATR-FTIR spectroscopy and spectroscopic imaging for the analysis of biopharmaceuticals. *Spectrochim. Acta Part A Mol. Biomol. Spectrosc.* **2020**, *241*, 118636. [[CrossRef](#)] [[PubMed](#)]
35. Bernard, P.; Andrieu, V.; Astolfi, D. Observer design for continuous-time dynamical systems. *Annu. Rev. Control* **2022**, *53*, 224–248. [[CrossRef](#)]
36. Bayen, T.; Rapaport, A.; Tani, F.Z. Improvement of performances of the chemostat used for continuous biological water treatment with periodic controls. *Automatica* **2020**, *121*, 109199. [[CrossRef](#)]
37. Wang, J.; Chae, M.; Beyene, D.; Sauvageau, D.; Bressler, D.C. Co-production of ethanol and cellulose nanocrystals through self-cycling fermentation of wood pulp hydrolysate. *Bioresour. Technol.* **2021**, *330*, 124969. [[CrossRef](#)] [[PubMed](#)]
38. Kumar, M.; Prasad, D.; Giri, B.S.; Singh, R.S. Temperature control of fermentation bioreactor for ethanol production using IMC-PID controller. *Biotechnol. Rep.* **2019**, *22*, e00319. [[CrossRef](#)] [[PubMed](#)]
39. Kurth, A.C.; Sawodny, O. Control of age-structured population dynamics with intra specific competition in context of bioreactors. *Automatica* **2023**, *152*, 110944. [[CrossRef](#)]
40. De Battista, H.; Jamilis, M.; Garelli, F.; Picó, J. Global stabilisation of continuous bioreactors: Tools for analysis and design of feeding laws. *Automatica* **2018**, *89*, 340–348. [[CrossRef](#)]
41. Grisolia, G.; Fino, D.; Lucia, U. Thermodynamic optimisation of the biofuel production based on mutualism. *Energy Rep.* **2020**, *6*, 1561–1571. [[CrossRef](#)]

Disclaimer/Publisher's Note: The statements, opinions and data contained in all publications are solely those of the individual author(s) and contributor(s) and not of MDPI and/or the editor(s). MDPI and/or the editor(s) disclaim responsibility for any injury to people or property resulting from any ideas, methods, instructions or products referred to in the content.